International Journal of Computing and Digital Systems
ISSN (2210-142X)
Int. J. Com. Dig. Sys. #, No.# (Mon-20..)

Design and Development of Shamrock leaf shaped fractal Antenna for WLAN/WiMAX applications

SatheeshKumar Palanisamy[1,*], Khalaf Ibrahim Osamah[2], Sameer Algburi[3], Habib Hamam[4]

[1]*Department of ECE, BMS Institute of Technology and Management, Bengaluru India-5600064, satheeshp@bmsit.in*
[2]*Department of Solar, Al-Nahrain Research Center for Renewable Energy, Al-Nahrain University, Jadriya, Baghdad, Iraq. usama81818@nahrainuniv.edu.iq*
[3]*Al-Kitab University, College of Engineering Techniques, sameer.algburi@uoalkitab.edu.iq*
[4] *Uni de Moncton, NB, 1EA 3E9, Canada Habib.Hamam@umoncton.ca*

[*]*Corresponding Author*

***Abstract*—** An innovative fractal shamrock leaf-shaped antenna with built-in filtering performance has been constructed utilising a stepped impedance resonator (SIR). For multi-band, uniformly polarised FR4 substrate functioning, an aperture-coupled slot patch antenna is in use. Portable electronics and fixed-location networks alike have made use of patch antennas. Patch antennas have traditionally suffered from limited gain, power handling, and impedance bandwidth. The proposed layout's primary goal is to employ filtering to dampen harmonics. Inherent advantages of the suggested design produce antennas that are both smaller in size and capable of operating over a wider frequency range. The multilayered fractal shamrock leaf shaped antenna is employed with a resonating frequency of 2.4GHz, 5.8 GHz, 3.5 GHz, 7.9GHz-ITU-R band with FR4 substrate. The SIR dual-band band pass filter is used to suppress the harmonics and reduce the dimension of the whole structure. The proposed antennas were fed by micro strip line and considered apertures coupling feeding techniques for suppressing harmonic frequencies and matching impedances. The number of iteration is varied, which in turn enhances the multiband characteristics. Both the measured and simulated results reveal improved radiation performances and bandwidth. The simulated outcome shows the better outcome in terms of gain and S11(dB)[reflection coeffeceint) i.e., for 2.4GHz (gain value of 3.3 dBi is attained with a S11(dB)[reflection coeffeceint) of -38 dB, for 3.5 GHz (the gain is 38 dBi having S11(dB)[reflection coeffeceint) of -26 dB), for 5.8 GHz (gain is 4.1 dBi with return values -32 dB), for 7.9GHz (the gain is 3.9 dBi having S11(dB)[reflection coeffeceint) of about -20.5 dB).. Thus, from the analysis, it is evident that the proposed design effectively suppresses the harmonics, thereby offering high impedance and better S11(dB)[reflection coeffeceint).

***Index Terms*—** multi-band fractal shamrock leaf shaped antenna, filtering, aperture-coupled slot, harmonics

1. INTRODUCTION

As the technology for wireless telecommunication improves, both the channel's carrying capacity and the data's throughput rate increase. By fine-tuning the service modes to be more adaptable, the compatibility across the various operating systems is improving, leading to ever-expanding operational bandwidth. Standards may be used in more and more systems simultaneously, from the GSM, PCS, DCS, and 4G tele communication; Using space-filling assets to realise the antenna's multiband while keeping its compact size is an innovative application of the fractal theory in antenna design that is analogous to the usage of self-similarity properties of the fractal body. To cite: Potapov et al. (2019)[1. With the growth of science and technology, the miniaturized size electronics and telecommunications equipment can perform varied functions more and more Jindal et al. (2019)[2]. In turn, this also leads to the antenna that other components must make them less significant Bai et al[3]. This technology also facilitates the integration of active modules directly and beam forming network with the radiating layers in phased and active arrays Zhou et al[4]. This aspiration might be attained with the use of a multilayer technique for the antenna construction by using electromagnetic coupling among the beam forming, radiating, and active layers Gupta et al[5]. So as to attain appropriate polarization, radiation efficiency, and other attributes over a specified frequency band, height, shape, dielectric substrate, and feeding arrangements of this planar radiator might be optimized Madhav et al[6]. This could be attained by the array

of several patches of the micro strip and through integrating signals established by them.

The fractal geometry is functional in several areas of life like medicine, computer science, art, biology, and so on, Naser-Moghadasi et al[7]. The fractals are theoretical objects, which cannot be implemented physically. On the other hand, some correlated geometries might be employed to approach an ideal fractal, which is valuable in the construction of antennas da Silva Junior et al[8]. Several significant fractal geometry characteristics were helpful in antennas designing having a multi-frequency operation and small size Zhangfang et al[9], Gupta et al[10].

In long-distance communications, the requirements of antenna property such as narrow beam-width and high gain can't be attained through a single patch structure. To avoid this lacuna, micro strip arrays were employed in most cases. As a result of employing fractal theory for these arrays, different radiation and multiband properties could also be attained.

The optimized in-sized fractal antennas and the performance were appropriate for wireless applications Harbadji et al[20]. Fractal Antenna Systems, Ficosa International and Ray span among others, investigate the distinctive property of fractals for the commercial antennas manufacturing.

A. Organization

The approach's residual part is systematically laid out in this section II, which depicts a variety of conventional approaches linked to fractal antennas. In Section III, we describe the proposed method (a fractal antenna design in the shape of a shamrock leaf), and in Section IV, we evaluate its performance. Section V provides the final analysis and verdict.

II. Related Works

Kwon et al. [11] demonstrated a small, high-resolution (3-D) antenna for use in the automobile industry. An inexpensive manufacturing procedure allowed for the antenna solution's planned shark-fin housing to be easily built from a PCB and a metal sheet.

For the WLAN/WiMAX application, Wang et al.[12] created a unique micro strip-fed antenna slot with a directed radiation pattern. A planar MIMO antenna was presented by Biswas et al.[13], which could be incorporated into the portable wireless device. We measured and talked about the antenna's properties, including its coefficient of reflection, gain, mutual coupling, and radiation pattern.

Results from experiments, analyses, and designs for high-gain models and reconfigurable antenna arrays were provided by Abdullah et al. [14]. The RF switches simplify the array pattern at degrees 0^0, 70^0, and 290^0 in the azimuth plane, providing high peak gain and narrowed altitude plane beam of width.

Ihamji et al.[15] analysed the uses of Radio Frequency Identification (RFID) readers and built a small, multiband rectangular micro strip antenna. CST Microwave Studio enhances the miniaturisation accomplished via fractal system and structures of physical parameters and its ground plane.

The low-cost fractal antenna design using parasitic SRR was presented by Sharma et al.[16]. EC Increased bandwidth is the result of better impedance matching, which is achieved thanks to parasitic SRR components. At 3.2 GHz, circular patch antenna is the simplest resonant structure to examine. The expected 13.3 dB gain using the modelled antenna agrees well with the measured and simulated results.

The Modified Sierpinski Carpet Fractal Antenna, as reported by Sivia et al.[17], is capable of resonating at a total of six different frequencies. The antenna is simulated in HFSS V13 by ANSYS/ANSOFT and is fed through a coaxial feed probe. The antenna provided here is very straightforward in design. The range of frequencies considered was from 1 GHz to 10 GHz.

For the use of numerous frequency bands, Elavarasi et al.[18] presented an SRR equipped with a Koch star fractal antenna. The CPW-Fed ant is made up of a CSRR marked on the bottom of the substrate and an iterated Koch star marked on the top of the FR4 layer. A 12 mm x 14 mm version of the Koch fractal SRR antenna was built and put through its paces for testing.

Patch antenna performance for wireless applications was evaluated by Desai et al.[19], who zeroed in on analysis and a hexagon design that stimulated fractal geometry and a defective ground plane.

A new dual-band miniaturized fractal antenna for wireless telecommunication use was developed by Harbadji et al.[20]. By placing square slots in the antenna's central ground, we may excite two resonant modes at once, the antenna's anticipated miniaturisation. A crescent-shaped fractal geometry was used by Chaouche et al.[21] to show a waveguide-fed, coplanar reconfigurable antenna. The suggested antenna is smaller than earlier reported constructions while yet providing the advantages of a multiband configuration.

Elavarasi et al[22] designed PWF shaped fractal patch supporting the multiband applications. The flower-shaped fractal patch was rigid on the substrate at which their proportions were $W_s \times L_s \times h$ mm^3 in addition to a ground was also customized (MG) for attaining the bands of multiple frequency.

III. Shamrock leaf shaped fractal antenna design

In this part of the paper, we discuss the suggested system and its underlying mechanism.

The multi-band fractal antenna design with filtering using stepped impedance resonator and harmonics suppression. The multilayered fractal shamrock leaf shaped antenna is employed with resonating frequency of 2.4GHz, 3.48 GHz, 5.78 GHz, 7.9GHz-ITU-R band with FR4 substrate.

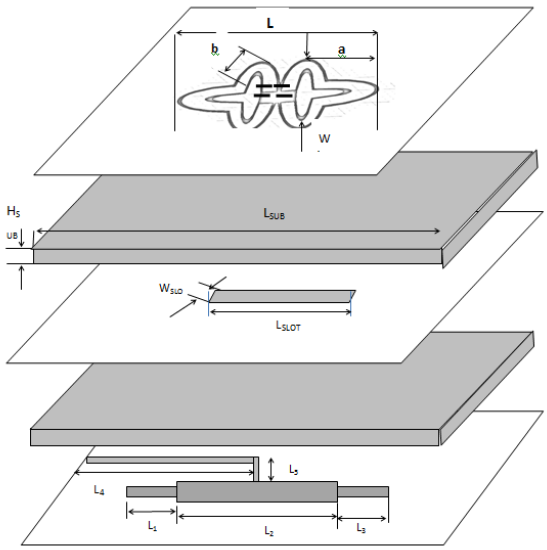

Figure 1 Layout of the Proposed Multi Band Filtering Antenna

Figure 1 is the representation of proposed multiband filtering antenna configuration.

A. Antenna Geometry

The proposed antenna design requires permittivity or dielectric of substrate and resonant frequency. The effectual dielectric constant ε_{eff} of the antenna is computed depending on the ratio of substrate's patch width (w) and thickness (h), either less than or greater than unity.

The thickness of the substrate provides a better antenna characteristics, and it depends on f_r. The thickness of the substrate lies between $0.003\ \lambda_0 < h < 0.05\ \lambda_0$.

$$\lambda 0 = \frac{c}{f_r} \quad (1)$$

The Length (L_{sub}) and Width (W_{sub}) of the substrate are calculated as follows

$$L_{sub} = 6h + L \quad (2)$$

$$W_{sub} = 6h + W \quad (3)$$

$$L_{eff} = L + 2\Delta L \quad (4)$$

Where,

h is the thickness and is 1.05

L is the patch's length and is 48nm

B. Design of rectangular patch

The aperture coupled feeding technique is employed in this approach at which the feed line is being separated fromthe use of the ground plane. The feed line and the radiating element are being coupled by means of slot or the aperture present in the ground plane. The coupling variation might depend on the slot's length and width for the enhancement of simulation outcome related to S11(dB)[reflection coeffeceint)es and bandwidths. Usually, the slot was centered at the resonating element.

Width of the rectangular shaped patch (W) is given as

$$W = \frac{c}{2f_0\sqrt{(\varepsilon_r+1)/2}} \quad (5)$$

Length of the rectangular shaped patch (L) is given as

$$L = \frac{c}{2f_0\sqrt{\varepsilon_{eff}}} - 0.824h\left[\frac{(\varepsilon_{eff}+0.3)*\left(\frac{W}{h}+0.264\right)}{(\varepsilon_{eff}-0.258)*\left(\frac{W}{h}+0.8\right)}\right] \quad (6)$$

$$\varepsilon_{eff} = \frac{\varepsilon_r+1}{2} + \frac{\varepsilon_r-1}{2}\left[\frac{1}{\sqrt{1+12\frac{h}{W}}}\right] \quad (7)$$

Where ε_{eff} = Effective dielectric permittivity

h = Thickness of the substrate

ε_r = Relative permittivity is 4.4 for FR4 material.

The below figure 2 is the representation of the rectangular patch.

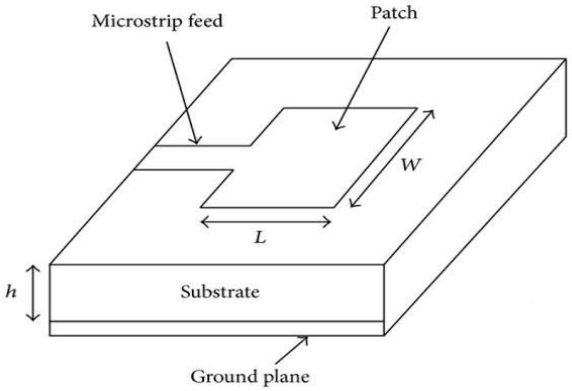

Figure 2 Rectangular patch

From the design calculation of patch, Width (W) of the patch is 58mm.Length of the substrate (L_{sub}) is 54nm, and the Width of the substrate (W_{sub}) is 64mm, ε_{eff} is 2.7.

.

C. Design of elliptical patch from the rectangular patch

Rectangular patch is designed as per the calculation of the length, width, and εeff. The elliptical patch is designed from a rectangular patch as per the equations given below.

The general equation of ellipse can be expressed as

$$\frac{X^2}{a^2} + \frac{Y^2}{b^2} = 1 \qquad (8)$$

Radiation fields in the elliptical patch antenna result in two orthogonal, equally-amplitude modes that are 90 degrees out of phase with one another. The feeding position lies on a line 45 degrees from the ellipse's major and minor axes. Fig. 3 represents flow diagram of elliptical shamerock leaf fractal antenna design, Fig. 4 shows the elliptical patch design.

Design of elliptical patch from the rectangular patch

The semi major axis radius of the elliptical patch is calculated as

$$\text{Semi major axis radius, a} = \frac{Length\ of\ rectangular\ patch(L)}{2} \qquad (9)$$

The semi minor axis radius of the elliptical patch is calculated as

$$\text{Semi minor axis radius, b} = \frac{Width\ of\ rectangular\ patch(W)}{2} \qquad (10)$$

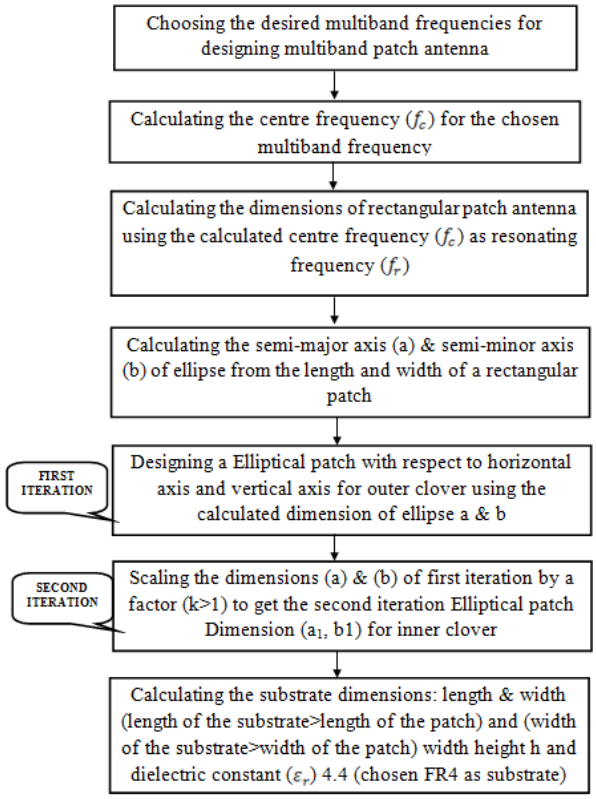

Figure 3 Flow of the proposed fractal antenna design

The desired multiband frequency is chosen for designing multiband patch antennas, and for this, the centre frequency is estimated. The rectangular patch antenna dimension is estimated using this computed center frequency as the resonating frequency. At the first iteration, elliptical patch is designed corresponding to the horizontal axis and vertical axis for the outer shamrock with the use of an estimated ellipse dimension. In the second iteration, the scaling of dimension in the first iteration is carried for attaining the elliptical patch dimension for the inner shamrock. At last, the substrate dimension is estimated with its length and width.

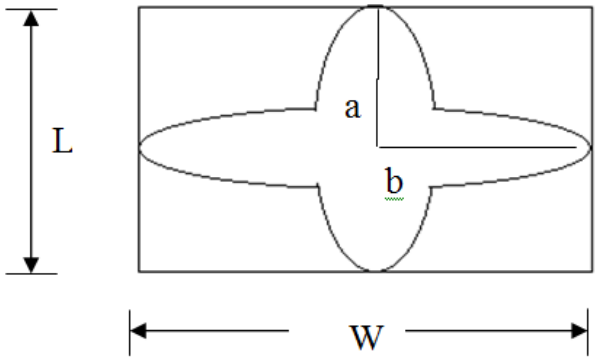

Figure 4 Elliptical patch design

The Design calculation is computed as follows with a as24nm and b as 29nm.

For the Different iterations, the flow of design is as follows:

Figure 5 Truncated elliptical ring

Figure 5 shows truncated elliptical ring, which used to construct the leaf-shaped patch. Truncated elliptical ring is designed by cutting two ellipses of the same ratio as 0.4 with the radius of 0.7 and 0.8 respectively.

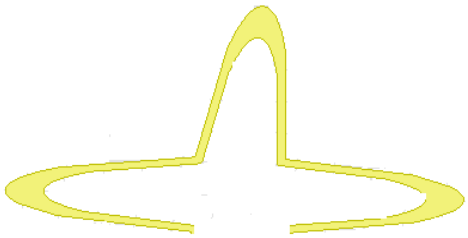

Figure 6 First iteration of patch

Figure 6 depicts the first iteration of the fractal patch. The first iteration is designed by combining the three truncated elliptical ring resembling a three shamrock leaf. The first iterated patch is duplicated by 180 degrees.

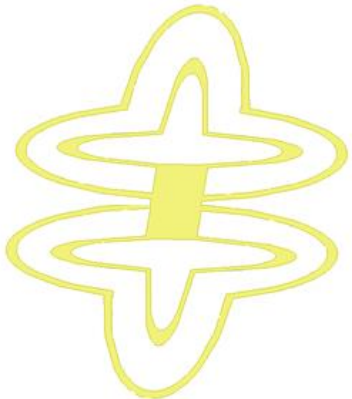

Figure 7 Second iteration of patch

Figure 7 represents the 2nd iteration of the fractal patch. The second iteration is designed by the length of the extracted ring at the previous section (first iteration), which is multiplied by a factor of 1.5.

D. Filter design:

Harmonics is a severe dilemma to be considered in the wireless communication system. Conventionally, harmonics were often eradicated by means of cascading a filter on the backend. On the other hand, this in turn enhances the volume of the RF front-end and complexity. In this incorporated antenna filtering, the harmonic suppression was considered.

Equivalent circuit of Stepped Impedance Filter Design

The given band pass filter has been obtained by using the following set of formulas and assumptions. The filter has been designed for an insertion loss of -30 dB, which helped in determining the filter order. Fig. 8(a) and (b) shows equivalent circuit of shamrock leaf shape antenna:

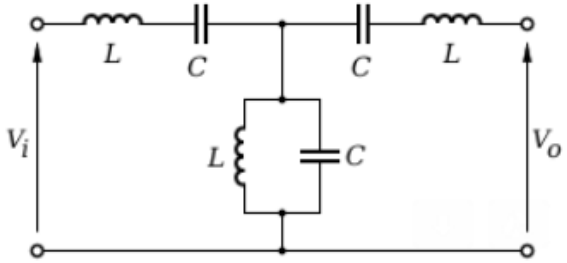

Figure 8 (a) Equivalent circuit of band pass filter design

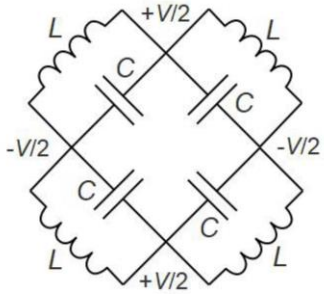

Figure 8 (b) Equivalent circuit of shamrock leaf shape antenna

Butterworth filters have been utilised to create the band pass filter, with their corresponding g employed to calculate the filter's L and C components and their respective impedance values. The formula for finding 'N' is shown below.

$$\text{Insertion Loss, } I_L = 10\log_{10}(1+\Omega^{2N}) \qquad (11)$$

Inductance (L=g*Z) is calculated by,

$$\bar{L} = \frac{L}{\omega_U - \omega_L} \ , \qquad (12)$$

$$\bar{C}=\frac{\omega_U-\omega_L}{\omega_0^2 L} \quad (13)$$

Capacitor(C=g/Z) in shunt is calculated by,

$$\bar{C}=\frac{C}{\omega_U-\omega_L} \quad ,\bar{L}=\frac{\omega_U-\omega_L}{\omega_0^2 C} \quad (14)$$

The following formula can be used to get the bandwidth factor of the filter being developed.

$$bf = \tan\left(\frac{\pi}{2}\left(1-\frac{s_{bw}}{2}\right)\right) \quad (15)$$

$$s_{bw}=\frac{\omega_U-\omega_L}{\omega_0^1}, \quad (16)$$

Inductive reactance (series inductor),

$$X= bf * g \quad (17)$$

Inductive susceptance (shunt capacitor),

$$B=bf * g \quad (18)$$

The stepped impedance resonator has two different characteristic impedance lines like Z_1 and Z_2. Y_{in1} is the input admittance from a different position. The input admittance (Y_{in}) of SIR is:

$$Y_{in} = \frac{(Z1 - Z2\tan\theta1\tan\theta2)}{[jZ1(Z1\tan\theta1 + Z2\tan\theta2)]} \quad (19)$$

The resonators dimensions could be derived just the once the band pass frequencies are discrete. The θ_1 electrical length is being determined through a range of structural parameters, together with L_1, L_2, L_3, L_4, and L_5, which in turn estimates the frequency value. It is appropriate for adjusting frequency by altering the L_5 value devoid of having much coupling coefficient influence.

Accordingly, the subsequent derivation could be attained as the condition of resonance:

$$\frac{z_1}{z_2} = tan\theta_1 tan\theta_2 = R_z \quad (20)$$

Where, R_z denotes the ratio of impedance. In this derivation, the resonance condition could be derived by means of θ_1, θ_2, and R_z. This could alter these factors so as to attain the required resonance, and the dual mode filter could be designed with the use of SIR.

The relationship between the electrical length of the SIR and the electrical length of the impedance Z_1, θ_1 are derived. When $0<R_z<1$, θ has a minimum value, and when $R_z>1$, θ has the maximum value. Fig. 9 shows Stepped Impedance Resonator structure.

$$\theta = tan^{-1}\sqrt{R_z} = \theta_1 = \theta_2 \quad (21)$$

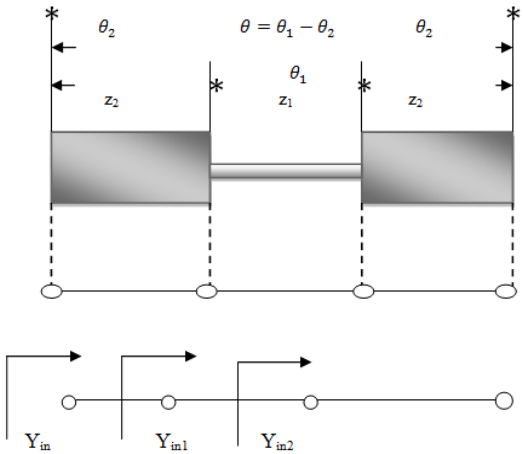

Figure 9 SIR structure

The filtering design of the antenna consists of half wavelength which has parallel coupled resonators, patch element, and the micro strip line feed. The centre inserted ground plane is shared by both filter and the patch antenna. During this design, whole structure's dimension can be reduced significantly.

IV. Performance Analysis

In this section, performance analysis was probable with the HFSS software simulation usage. The comparative analysis Mao et al[23] of the proposed and existing mechanism is shown. Fig. 10 symbolises the 1st iteration of the proposed fractal. Fig.11 shows the 2nd iteration of fractal antenna by incorporating inner shamerock leaf.

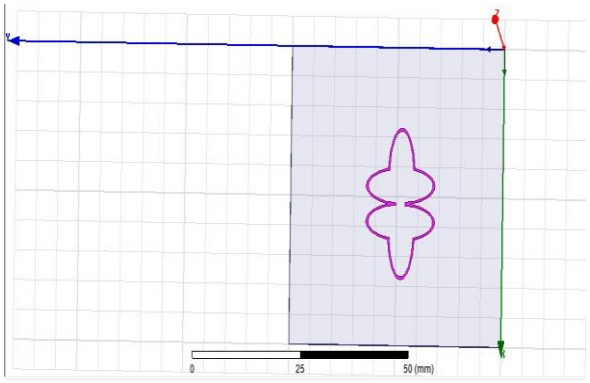

Figure 10 Representation of First iteration (top view-fractal patch)

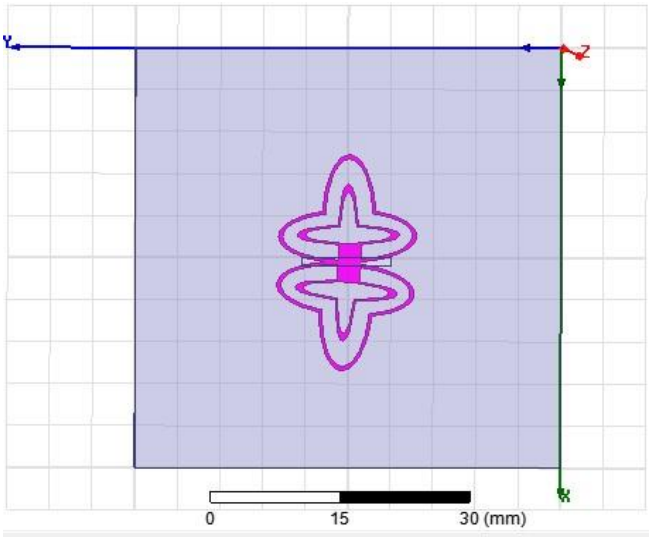

Figure 11 Representation of Second iteration (top view)

From the design of leaf shamrock antennas, patch antennas have been employed. Figure 12 shows the patch antennas having the shape of the shamrock of petals that were operating in the WLAN range.

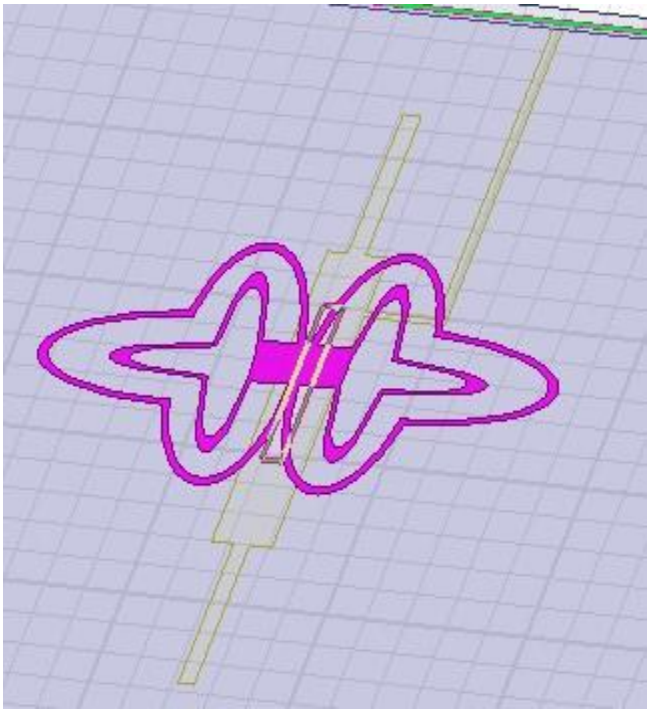

Figure 12 representation of Second iteration with filter

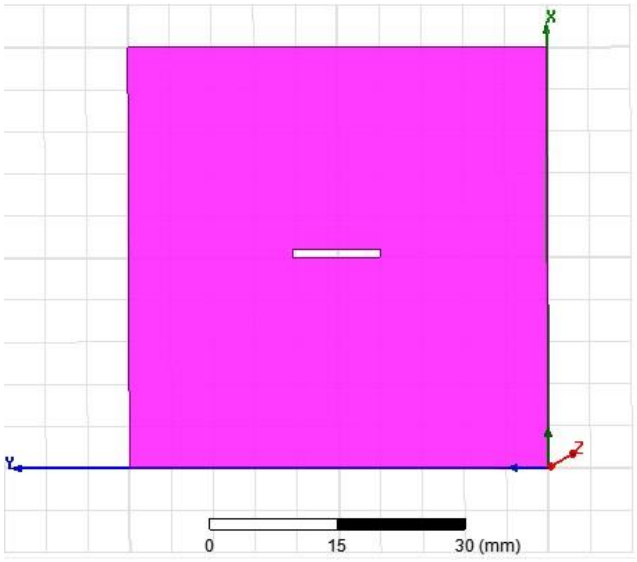

Figure 13 Slot at ground plane to support proximity coupling

Figure 13 represents slot at the middle ground plane to support proximity coupling feeding technique. Figure 14 is the Second order Stepped impedance resonator at the bottom layer to suppress harmonics other than 2.48 GHz, 5.78 GHz (WLAN) application), 3.5 GHz (WiMAX), 7.9 GHz-ITU-R band.

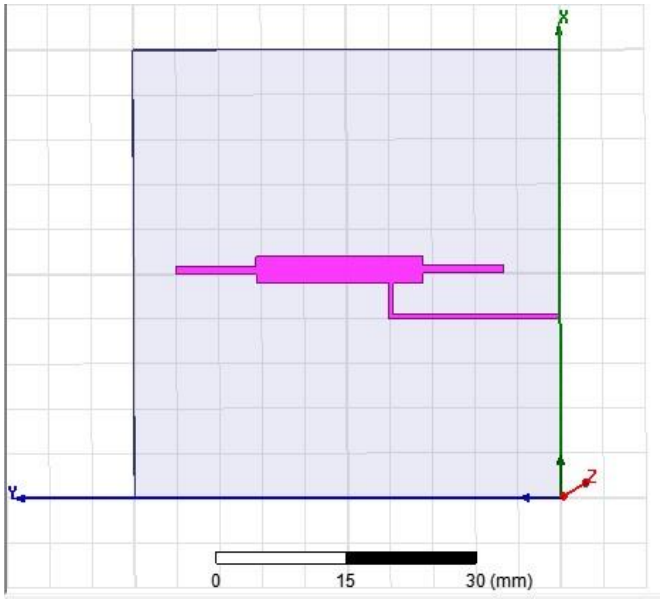

Figure 14 representation of First iteration (Top view)

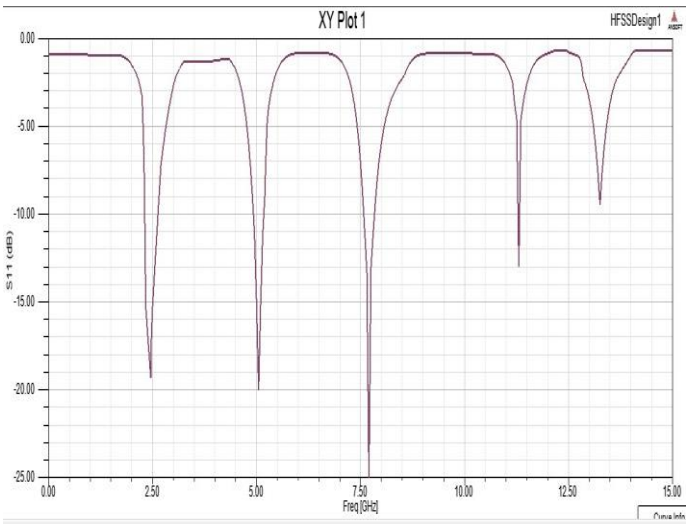

Figure 15 S11(dB)[reflection coeffeceint) analysis of first iteration

Figure 15 signifies S11(dB)[reflection coeffeceint) (S_{11}) of first iteration of fractal without filter resonating at 2.49 GHz, 7.6GHz, and harmonics at 5 GHz, 11.2 GHz, and 13.2 GHz.

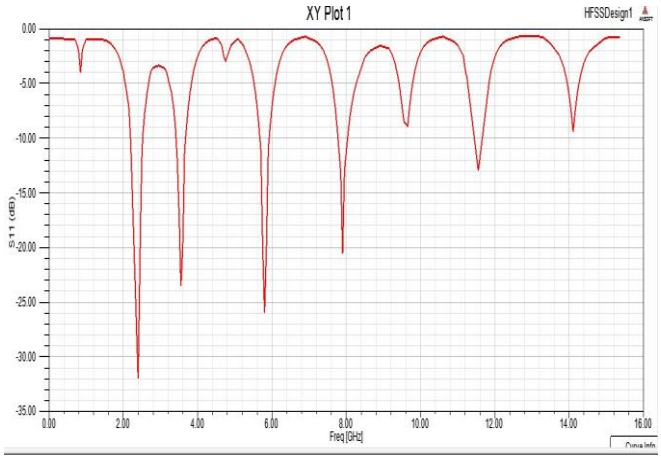

Figure 16 $_{S11}$(dB)[reflection coeffeceint) analysis of second iteration

Figure 16 symbolises the S_{11}(dB)[reflection coeffeceint) of second iteration without filter resonating at 2.4 GHz, 3.5GHz, 5.8GHz, 7.9GHz (desired radiating frequencies) and other radiating frequencies are Harmonics, which have to be suppressed.

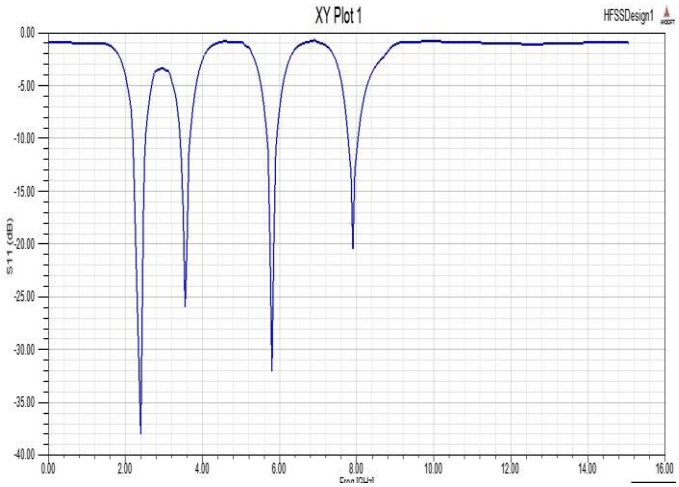

Figure 17 Filtered S_{11}(dB)[reflection coeffeceint) analysis of second iteration

The analysis of Filtered S_{11}(dB)[reflection coeffeceint) of second iteration is shown in figure 17, which is resonating at 2.4 GHz, 3.5GHz, 5.8GHz, 7.9GHz (desired radiating frequencies) and no harmonics.

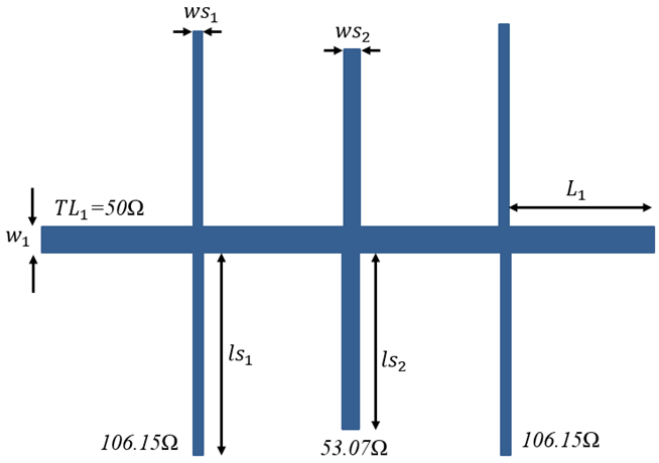

Figure.5 Impedance and width modified BPF

Table.1 Dimensional parameters of the impedance and width modified BPF

Impedance(Ω)	Parameter	Value(mm)
50	W1	2.93310
	L1	8.217530
106.15	ls_1	35.0144
	ws_1	0.523472
53.07	ls_2	33.0357
	ws_2	2.64502

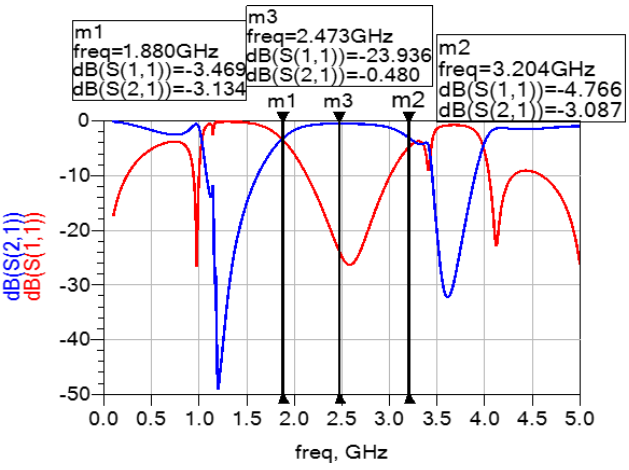

Figure 19 Filtered S_{11}(dB)[reflection coeffeceint) and S_{21}(dB)[transmission Coeffecent] analysis of proposed filter

Figure 18 is the analysis of the Stepped Impedance Resonator, which generates two-second order bands (dual band: 1.8GHz-3.7 GHz) & (5.22GHz – 8GHz).

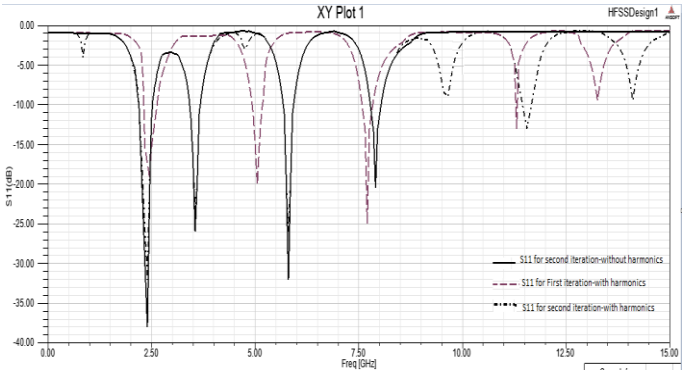

Figure 19 comparative analyses of second iteration with and without filter and first iteration

The Comparative result is shown in figure 19 in which Solid line signifies second iteration with filter-only desired radiating frequencies and Red-long dotted: second iteration without filter. The Blue dotted indicates the First iteration.

Once the RF front end system has been installed, the effect of the ground plane can be taken into account. No matter what you do to the ground plane, the out-of-band and in-band performance won't change. This proposed design features low insertion and in-band S_{11}(dB)[reflection coeffeceint).

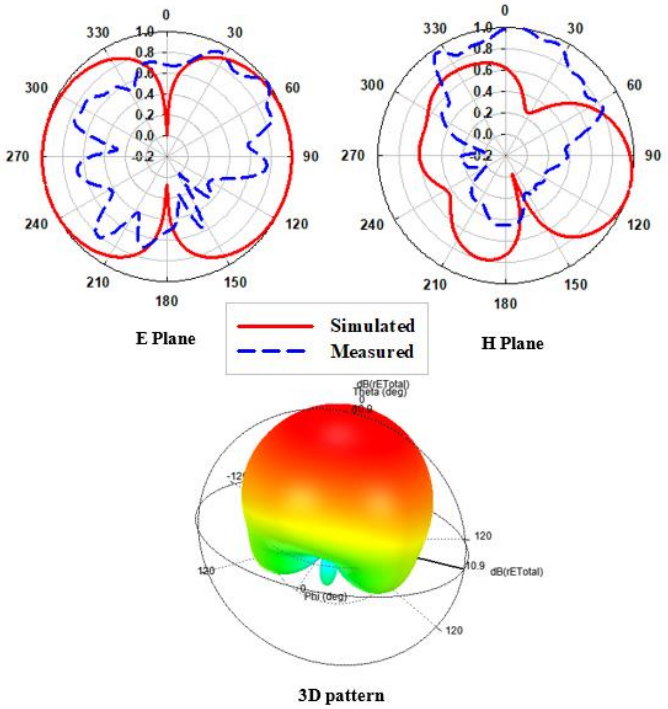

Figure 20 Analysis of radiation pattern(E-plane and H-plane) at 2.4 GHz and 3.6 GHz

Radiation pattern (E Plane (dB))- phi in degree Vs Gain is shown in figure 20 in which solid line signifies 2.4 GHz with Dotted line of 3.5 GHz.

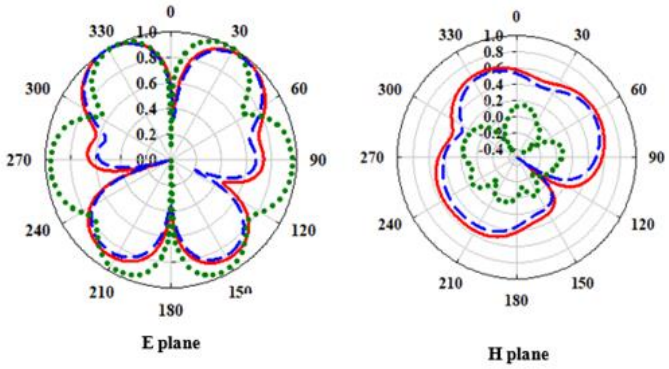

Figure 21 Analysis of 2D-radiation pattern(E-plane and H-plane) at 7.9 GHz and 5.8 GHz

Radiation pattern (E Plane (dB)) - phi in degree Vs Gain is shown in figure 21 in which solid line: 7.9 GHz and Dotted line: 5.8 GHz. The radiation patterns are stable and Omni-directional over the whole pass band. The outcomes of the filtering antenna were close to one another which in turn validates the effectiveness of the proposed design.
The simulated gain (dB) in the resonant frequencies of the patch antennas is shown. As renowned, the gain was condensed when fractal level increases.

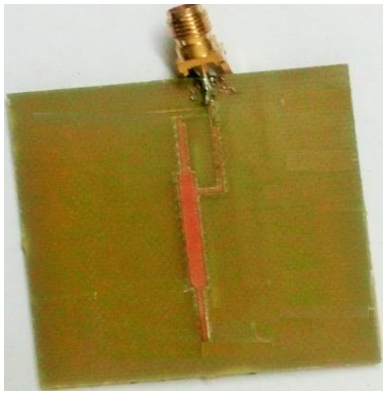

Figure 22 Bottom view of fabricated shamrock shaped fractal antenna design

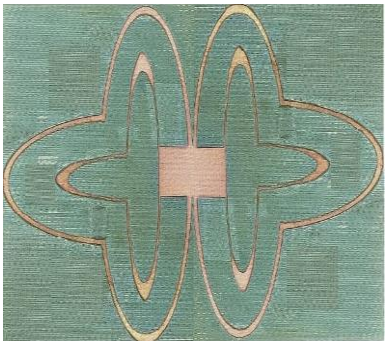

Figure 23 Top view of fabricated shamrock shaped fractal antenna design

Figure 22 is the representation of the bottom view of fabricated shamrock shaped fractal antenna design, and figure 23 is the top view of fabricated shamrock shaped fractal antenna design.

Table 1 performance analysis of the gain vs. resonant frequency

	Gain, S11(dB)[reflection coeffeceint) vs. resonant frequency							
Iteration	2.48 GHz		3.48 GHz		5.8 GHz		7.9 GHz	
	Gain (dbi)	S_{11} (dB)	Gain (dBi)	S_{11} (dB)	Gain (dBi)	S_{11} (dB)	Gain (dBi)	S_{11} (dB)
2nd iteration with filter	3.3	-38	3.8	-26	4.1	-32	3.9	-20.5
2nd iteration without filter	3.25	-32	3.7	-23.48	3.5	-26	3.7	-20.5
1st iteration	3.0	-19.2	3.2	-1.1418	3.0	-0.96155	3.1	-2.75

Table 2 comparative analysis of the simulated and fabricated result

Simulated result		Fabricated result	
Frequency	**dB**	**Frequency**	**dB**
2.4 GHz	-38	2.4GHz	-36
3.5 GHz	-26	3.5 GHz	--28
5.8 GHz	--32	5.8 GHz	-30.5
7.9 GHz	-20.5	7.9 GHz	-19.8

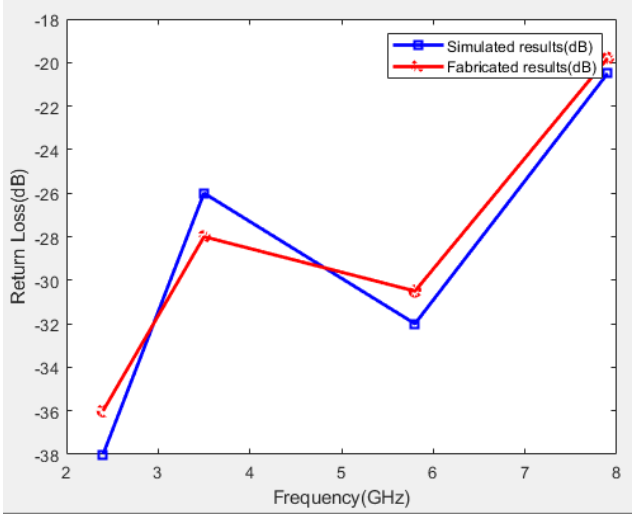

The proposed system's performance analysis is displayed in Table 1 in terms of gain and resonant frequency. The comparison between the simulated and constructed results is shown in Figure 24 and Table 2.

Table 3 Comparison of S_{11}(dB)[reflection coeffeceint), Gain and Radiating Efficiency of Existing Conventional Multiband antenna and proposed antenna

	Gain, S_{11}(dB)[reflection coeffeceint) and Radiating Efficiency vs. resonant frequency											
Iteration	2.4 GHz			3.5 GHz			5.8 GHz			7.9 GHz		
	Gain (dbi)	S_{11} (dB)	Radiating efficiency (in %)	Gain (dBi)	S_{11} (dB)	Radiating efficiency (in %)	Gain (dBi)	S_{11} (dB)	Radiating efficiency (in %)	Gain (dBi)	S_{11} (dB)	Radiating efficiency (in %)
Proposed Antenna	3.3	-38	94.6	3.8	-26	92.4	4.1	-32	90.5	3.9	-20.5	91.6
Existing Conventional Multiband antenna	2.8	-28	90.2	3.2	-16.8	89.1	3.4	-25	91.2	2.8	-25	89.5

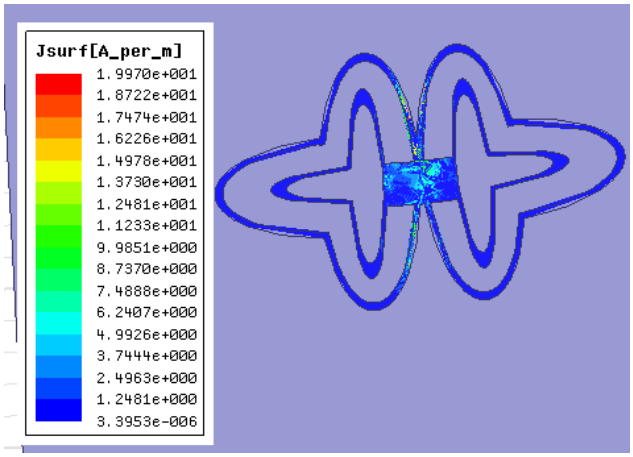

Figure 25 Surface current Distribution at 2.4 GHZ, 3.5 GHz, 5.8 GHz, and 7.9GHz

Table 3 depicts the Comparison of S11(dB)[reflection coeffeceint), Gain and Radiating Efficiency of Existing Conventional Multiband antenna and proposed antenna. The outcome shows that the proposed design is better than the existing techniques. Figure 25 is the representation of surface current distribution at 2.4 GHZ, 3.5 GHz, 5.8 GHz, and 7.9GHz.

V. Conclusion

This article demonstrated the designing of inventive multilayered fractal-shamrock leaf shaped antenna for the wireless application. The antenna is being designed with the FR4 substrate having a resonating frequency of value 2.48 GHZ, 5.8 GHz(WLAN) application), 3.48 GHz (Wi-Max), 7.9 GHz-ITU-R band as a top patch as the technique of feeding aperture coupling slot probe has been utilized as the antenna feed in the ground plane. The bottom band patch as Stepped Impedance Resonator, which in turn generates two second order bands (dual band: 1.8GHz-3.7 GHz) and (5.22G–8GHz). The main aim of this design is to suppress the harmonics by multi-band fractal antenna having filtering with the use of a stepped impedance resonator. The simulated result shows the better outcome in terms of gain and S_{11}(dB)[reflection coeffeceint) i.e. for 2.4GHz (gain of 3.3 dBi is attained with a S_{11}(dB)[reflection coeffeceint) of -38 dB), for 3.5 GHz (the gain is 38 dBi having S_{11}(dB)[reflection coeffeceint) of -26 dB), for 5.8 GHz (gain is 4.1 dBi with return values -32 dB), for 7.9GHz (the gain is 3.9 dBi having S_{11}(dB)[reflection coeffeceint) of about -20.5 dB).

Conflict of Interest

The authors declares no conflict of interest

Funding

The authors thank Natural Sciences and Engineering Research Council of Canada (NSERC) and New Brunswick Innovation Foundation (NBIF) for the financial support of the global project. These granting agencies did not contribute in the design of the study and collection, analysis, and interpretation of data.

REFERENCES

[1] A. Potapov, "Fractal Electrodynamics: Numerical Modeling of Small Fractal Antenna Devices and Fractal 3D Microwave Resonators for Modern Ultra-Wideband or Multiband Radio Systems," Journal of Communications Technology and Electronics, vol. 64, pp. 629-663, 2019.

[2] S. Jindal, J. S. Sivia, and H. S. Bindra, "Hybrid fractal antenna using meander and Minkowski curves for wireless applications," Wireless Personal Communications, vol. 109, pp. 1471-1490, 2019.

[3] X. Bai, J.-w. Zhang, and L.-j. Xu, "A broadband CPW fractal antenna for RF energy harvesting," in 2017 International Applied Computational Electromagnetics Society Symposium (ACES), 2017, pp. 1-2.

[4] Z. Zhou, W. Liao, Q. Zhang, F. Han, and Y. Chen, "A multi-band fractal antenna for RF energy harvesting," in 2016 IEEE International Symposium on Antennas and Propagation (APSURSI), 2016, pp. 617-618.

[5] A. Gupta, H. D. Joshi, and R. Khanna, "An X-shaped fractal antenna with DGS for multiband applications," International Journal of Microwave and Wireless Technologies, vol. 9, p. 1075, 2017.

[6] B. Madhav and T. Anilkumar, "Design and study of multiband planar wheel-like fractal antenna for vehicular communication applications," Microwave and Optical Technology Letters, vol. 60, pp. 1985-1993, 2018.

[7] M. Naser-Moghadasi, R. A. Sadeghzadeh, R. Khajeh Mohammad Lou, B. S. Virdee, and T. Aribi, "Semi fractal three leaf shamrock-shaped CPW antenna for triple band operation," International Journal of RF and Microwave Computer-Aided Engineering, vol. 25, pp. 413-418, 2015.

[8] P. F. da Silva Junior, M. S. P. Silva Filho, E. E. de Carvalho Santana, P. H. da Fonseca Silva, E. E. C. de Oliveira, M. A. de Oliveira, et al., "Fractal and Polar Microstrip Antennas and Arrays for Wireless Communications," in Wireless Mesh Networks-Security, Architectures and Protocols, ed: IntechOpen, 2019.

[9] H. Zhangfang, X. Wei, L. Yuan, H. Yinping, and Z. Yongxin, "Design of a modified circular-cut multiband fractal antenna," The Journal of China Universities of Posts and Telecommunications, vol. 23, pp. 68-75, 2016.

[10] M. Gupta and V. Mathur, "Wheel shaped modified fractal antenna realization for wireless communications," AEU-International Journal of Electronics and Communications, vol. 79, pp. 257-266, 2017.

[11] O.-Y. Kwon, R. Song, and B.-S. Kim, "A fully integrated shark-fin antenna for MIMO-LTE, GPS, WLAN, and WAVE applications," IEEE Antennas and Wireless Propagation Letters, vol. 17, pp. 600-603, 2018.

[12] H. Wang, L. Liu, Z. Zhang, Y. Li, and Z. Feng, "A wideband compact WLAN/WiMAX MIMO antenna based on dipole with V-shaped ground branch," IEEE Transactions on Antennas and Propagation, vol. 63, pp. 2290-2295, 2015.

[13] A. Biswas and V. R. Gupta, "Design and Development of Low Profile MIMO Antenna for 5G New Radio Smartphone Applications," Wireless Personal Communications, pp. 1-12, 2019.

[14] M. I. Abdullah, M. M. Rahman, and M. C. Roy, "Detecting sinkhole attacks in wireless sensor network using hop count," Int. J. Comput. Netw. Inf. Secur, vol. 3, pp. 50-56, 2015.

[15] M. Ihamji, E. Abdelmounim, H. Bennis, M. Hefnawi, and M. Latrach, "Design of compact tri-band fractal antenna for RFID readers," International Journal of Electrical and Computer Engineering, vol. 7, p. 2036, 2017.

[16] V. Sharma, N. Lakwar, N. Kumar, and T. Garg, "Multiband low-cost fractal antenna based on parasitic split ring resonators," IET Microwaves, Antennas & Propagation, vol. 12, pp. 913-919, 2017.

[17] J. S. Sivia, G. Kaur, and A. K. Sarao, "A modified sierpinski carpet fractal antenna for multiband applications," Wireless Personal Communications, vol. 95, pp. 4269-4279, 2017.

[18] C. Elavarasi and T. Shanmuganantham, "Multiband SRR loaded Koch star fractal antenna," Alexandria engineering journal, vol. 57, pp. 1549-1555, 2018.

[19] A. Desai, T. K. Upadhyaya, R. H. Patel, S. Bhatt, and P. Mankodi, "Wideband high gain fractal antenna for wireless applications," Progress In Electromagnetics Research, vol. 74, pp. 125-130, 2018.

[20] M. Harbadji, T. A. Denidni, and A. Boufrioua, "Miniaturized dual-band fractal antenna with omnidirectional pattern for WLAN/WiMAX applications," Progress In Electromagnetics Research, vol. 70, pp. 31-38, 2017.

[21] Y. B. Chaouche, I. Messaoudene, I. Benmabrouk, M. Nedil, and F. Bouttout, "Compact coplanar waveguide-fed reconfigurable fractal antenna for switchable multiband systems," IET Microwaves, Antennas & Propagation, vol. 13, pp. 1-8, 2018.

[22] C. Elavarasi and T. Shanmuganantham, "SRR loaded periwinkle flower shaped fractal antenna for multiband applications," Microwave and Optical Technology Letters, vol. 59, pp. 2518-2525, 2017.

[23] C. X. Mao, S. Gao, Y. Wang, B. Sanz-Izquierdo, Z. Wang, F. Qin, et al., "Dual-band patch antenna with filtering performance and harmonic suppression," IEEE Transactions on Antennas and Propagation, vol. 64, pp. 4074-4077, 2016.

[24] Iqbal Jebril & P. Dhanaraj & Ghaida Muttashar Abdulsahib & SatheeshKumar Palanisamy & T.Prabhu & Osamah Ibrahim Khalaf, 2022. "Analysis of Electrically Couple SRR EBG Structure for Sub 6 GHz Wireless Applications," Advances in Decision Sciences, Asia University, Taiwan, vol. 26(Special), pages 102-123, December.

[25] E. Suganya, T. Prabhu, Satheeshkumar Palanisamy, Praveen Kumar Malik, Naveen Bilandi, Anita Gehlot, "An Isolation Improvement for Closely Spaced MIMO Antenna Using λ/4 Distance for WLAN Applications", International Journal of Antennas and Propagation, vol. 2023, Article ID 4839134, 13 pages, 2023. https://doi.org/10.1155/2023/4839134.

[26] Xue, X.; Shanmugam, R.; Palanisamy, S.; Khalaf, O.I.; Selvaraj, D.; Abdulsahib, G.M.A Hybrid Cross Layer with Harris-Hawk-Optimization-Based Efficient Routing for Wireless Sensor Networks. *Symmetry* 2023, *15*, 438.https://doi.org/10.3390/sym15020438.

[27] A. P. Mukti, L. Lusiana, D. Titisari, and S. Palanisamy, "Performance Analysis of Twelve Lead ECG Based on Delivery Distance Using Bluetooth Communication", j.electron.electromedical.eng.med.inform, vol. 5, no. 1, pp. 46-52, Jan. 2023.

[28] AngurajKandasamy, SaravanakumarRengarasu, Praveen KittiBurri, SatheeshkumarPalanisamy, K. Kavin Kumar, Aruna Devi Baladhandapani, Samson AlemayehuMamo, "Defected Circular-Cross Stub Copper Metal Printed Pentaband Antenna", Advances in Materials Science and Engineering, vol. 2022, Article ID 6009092, 10 pages, 2022. https://doi.org/10.1155/2022/6009092.

[29] Sam P.J.C., Surendar U., Ekpe U.M., Saravanan M., Satheesh Kumar P. (2022) A Low-Profile Compact EBG Integrated Circular Monopole Antenna for Wearable

Medical Application. In: Malik P.K., Lu J., Madhav B.T.P., Kalkhambkar G., Amit S. (eds) Smart Antennas. EAI/Springer Innovations in Communication and Computing.Springer, Cham.https://doi.org/10.1007/978-3-030-76636-8_23.

[30] Satheesh Kumar, P., Jeevitha, Manikandan (2021). Diagnosing COVID-19 Virus in the Cardiovascular System Using ANN. In: Oliva, D., Hassan, S.A., Mohamed, A. (eds) Artificial Intelligence for COVID-19. Studies in Systems, Decision and Control, vol 358.Springer, Cham.https://doi.org/10.1007/978-3-030-69744-0_5.

[31] S, D.; Palanisamy, S.; Hajjej, F.; Khalaf, O.I.; Abdulsahib, G.M.; S, R. Discrete Fourier Transform with Denoise Model Based Least Square Wiener Channel Estimator for Channel Estimation in MIMO-OFDM. Entropy 2022, 24, 1601. https:// doi.org/10.3390/e24111601.

[32] Palanisamy, S, Thangaraju, B. Design and analysis of clover leaf-shaped fractal antenna integrated with stepped impedance resonator for wireless applications. Int J Commun Syst. 2022; 35(11):e5184. doi:10.1002/dac.5184.

[33] Nivethitha, T., Palanisamy, S. K., MohanaPrakash, K., &Jeevitha, K. (2021).Comparative study of ANN and fuzzy classifier for forecasting electrical activity of heart to diagnose Covid-19. Materials today. Proceedings, 45, 2293–2305. https://doi.org/10.1016/j.matpr.2020.10.400.

[34] Palanisamy, Satheeshkumar, BalakumaranThangaraju, Osamah Ibrahim Khalaf, YouseefAlotaibi, SalehAlghamdi, and FawazAlassery. 2021. "A Novel Approach of Design and Analysis of a Hexagonal Fractal Antenna Array (HFAA) for Next-Generation Wireless Communication" Energies 14, no. 19: 6204. https://doi.org/10.3390/en14196204.

[35] Palanisamy S, Thangaraju B, Khalaf OI, Alotaibi Y, Alghamdi S. Design and Synthesis of Multi-Mode Bandpass Filter for Wireless Applications. Electronics. 2021; 10(22):2853. https://doi.org/10.3390/electronics10222853.

[36] SatheeshKumar & Balakumaran T. (2021). Modeling and simulation of dual layered U-slot multiband microstrip patch antenna for wireless applications. Nanoscale Reports, 4(1), 15 – 18. https://doi.org/10.26524/nr.4.3.

[37] Palanisamy, S. (2022).Predictive Analytics with Data Visualization. Journal of Ubiquitous Computing and Communication Technologies, 4(2), 75-96. doi:10.36548/jucct.2022.2.003.

[38] Palanisamy, S., Rubini, S.S., Khalaf, O.I. et al. Multi-objective hybrid split-ring resonator and electromagnetic bandgap structure-based fractal antennas using hybrid metaheuristic framework for wireless applications. Sci Rep 14, 3288 (2024). https://doi.org/10.1038/s41598-024-53443-z